



Pergamon

Tetrahedron: Asymmetry 9 (1998) 4043–4054

TETRAHEDRON:
ASYMMETRY

New amidophosphine-phosphinites (tLANOPs) as chiral ligands for asymmetric hydrogenation reactions

Emil A. Broger, Wolfgang Burkart, Michael Hennig, Michelangelo Scalone* and Rudolf Schmid

Pharmaceuticals Division, Process Research and Structural Research, F. Hoffmann-La Roche AG, CH-4070 Basel, Switzerland

Received 5 October 1998; accepted 20 October 1998

Abstract

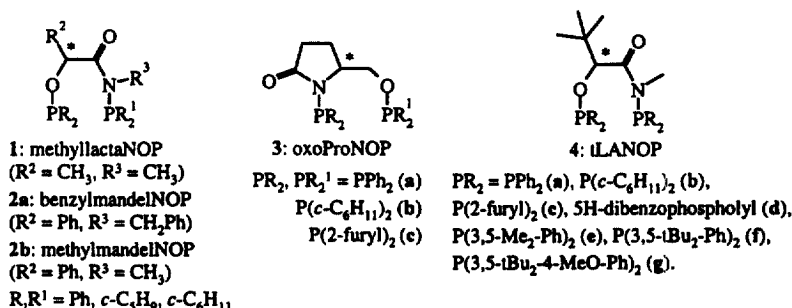
The new amidophosphine-phosphinite (AMPP) ligands **4a–g** (called tLANOP ligands) derived from the chiral hydroxy amide (*R*)- or (*S*)-2-hydroxy-3,3,*N*-trimethylbutyramide have been prepared in 48–83% yield. The crystal structures of the square planar complexes [(*SP*-4-3)-Pd((*R*)-dmphea)((*S*)-**4a**)]BF₄ and [Rh((*R*)-**4a**)(COD)]BF₄ have allowed the absolute configurations of the ligands to be assigned. In both complexes the 7-membered chelating ring of **4a** has virtually the same twist-boat conformation. With this class of ligands the rhodium catalyzed asymmetric hydrogenation of 4-oxoisophorone enol acetate gave (*S*)-phorenol acetate in up to 71% ee. The iridium catalyzed asymmetric hydrogenation of the cyclic iminium salts **16a** and **16b** afforded after work-up the corresponding cyclic secondary amine (*S*)-**17** in up to 86% ee, when bulky groups were present on the phenyl substituents on the two phosphorus atoms. © 1998 Elsevier Science Ltd. All rights reserved.

1. Introduction

Recently, amidophosphine-phosphinite (AMPP) ligands of formula **1–3** have been reported to give efficient asymmetric catalysts for the hydrogenation of α -functionalized ketones^{1,2} or allylic alcohols.³ These ligands are particularly interesting from a practical point of view because they can be prepared in very few steps from easily available natural products. Ligands of type **3** are derived from oxoprolinol and contain the carbonyl group in exocyclic position with respect to the 7-membered chelate ring formed after coordination to a transition metal. They have so far been the most effective in the asymmetric hydrogenation of, for example, dihydro-4,4-dimethyl-2,3-furandione, affording (*S*)-pantolactone of 95–99% ee.⁴ The ligands of type **1** and **2**, which have the carbonyl group endocyclic after

* Corresponding author. E-mail: michelangelo.scalone@roche.com

coordination to the metal, have afforded (*S*)-pantolactone in 81–90% ee. The lower enantioselectivity was ascribed to the lower rigidity of the backbone.^{1,4}



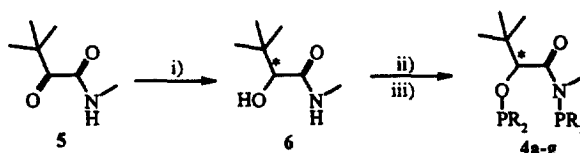
We reasoned that the 7-membered chelate ring could be made more rigid by replacing the methyl or the phenyl substituent of **1** or **2** by a *t*-butyl group. Indeed, molecular modelling calculations on cationic rhodium complexes supported this hypothesis. Moreover, they indicated that, after coordination to a metal, the chelate ring of **3a** and **4a** as well as **3b** and **4b** would have very similar preferred twist-boat conformations, thus suggesting a similar rigidity of the backbone in these two ligand families.⁵ Consequently, we have synthesized the new tLANOP ligands **4a–g** and tested them in two asymmetric hydrogenation reactions.

2. Results and discussion

2.1. Synthesis and characterization of the tLANOP ligands

The starting hydroxy amides (*R*)- and (*S*)-**6** were prepared by asymmetric hydrogenation of the ketoamide **5** in the presence of chiral ruthenium catalysts (Scheme 1).⁶ After crystallization they were isolated in 99% ee. Their absolute configuration was provisionally assigned by applying the general sense of the asymmetric induction observed in the BINAP–Ru catalyzed hydrogenation of α -functionalized ketones ((*R*)-BINAP gives (*R*)-alcohols)^{7,8} and was confirmed by determination of the crystal structure of the two complexes (*R,S*)-**10** and (*R*)-**13a** (vide infra). Then, the reaction of the dilithium salt of **6** with 2.1 molar equiv. of a chlorophosphine gave the tLANOP ligands **4a–g** in 48–83% yield. These phosphinylations proceeded selectively when BuLi was used in combination with a small amount (5%) of a secondary amine (e.g. diisopropylamine). This avoided the intermediate precipitation of an insoluble species, probably a monolithium salt of **6**, and suppressed almost completely the concomitant formation of by-products such as the diphosphine **7** and the *n*-butyl phosphine **8**. If a stoichiometric amount of diisopropylamine was employed, the phosphinylation was incomplete and substantial amounts of (*i*Pr₂N)PPh₂ were formed as a by-product. No formation of the desired ligands **4** was observed when **6** was treated in analogy to the procedures reported for **1–3**^{1,2,4} with a chlorophosphine in the presence of a Et₃N or DBU. Specifically, with Ph₂PCl, rapid monophosphinylation at the oxygen atom was observed at rt, but prolonged reaction times led only to formation of unidentified by-products. Under the same conditions, no reaction at all was observed with Cy₂PCl. Attempts to react the lithium salt of the monophosphinylated species with Cy₂PCl led only to complex mixtures of products.

The ligands **4a–g** are white, air-sensitive solids which can be stored without decomposition for months at rt under an argon atmosphere. They have been characterized by ¹H, ³¹P NMR and IR spectroscopy, microanalysis and mass spectrometry. Their NMR spectra are similar to those reported earlier for

i) $[\text{RuCl}_2((R)\text{- or } (S)\text{-BIPHEMP})]$, 60 bar H_2 , 60°C , 20 hii) BuLi , $i\text{Pr}_2\text{NH}$, THF, -78°C iii) 2 PR_2Cl , -78°rt , by-products: $(\text{R}_2\text{P})_2$ (7), $\text{R}_2\text{P-Bu}$ (8)

Scheme 1.

Table 1

Yields and $^{31}\text{P}\{^1\text{H}\}$ NMR data for the tLANOP ligands 4a–g

ligand	no.	yield (%)	$\delta(\text{P-N})$	$\delta(\text{P-O})$
Ph-tLANOP	4a	67	52.5	115.7
Cy-tLANOP	4b	69	65.4	139.3
(2-Furyl)-tLANOP	4c	48	0.8	64.9
(Diphol)-tLANOP	4d	62	40.4	112.1
(3,5-Xyl)-tLANOP	4e	73	53.3	117.7
(3,5- <i>t</i> Bu)-tLANOP	4f	83	56.4	112.4
(3,5- <i>t</i> Bu,4-MeO)-tLANOP	4g	60	54.2	110.8

the AMPP ligands 1–3.⁴ The two ^{31}P resonances were assigned accordingly: the P(N) and the P(O) resonances appeared at 40–65 ppm and 110–139 ppm, respectively, with the exception of (2-furyl)-tLANOP 4c, where the signals are shifted strongly upfield (Table 1).⁹

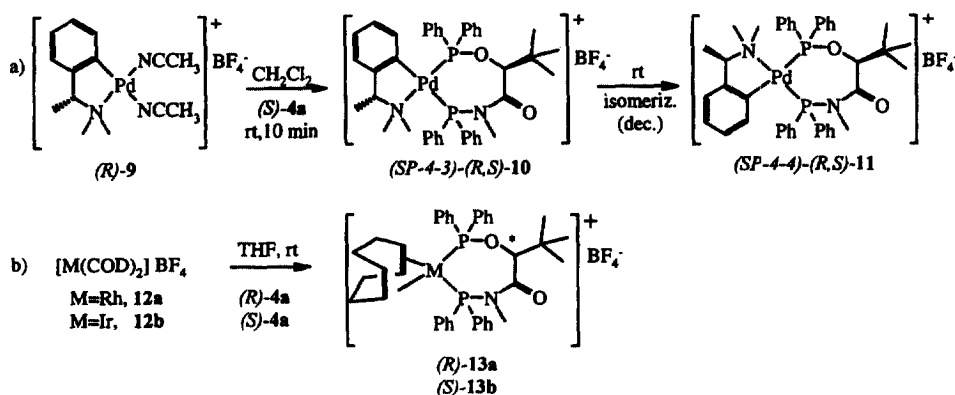
Since alcohols are employed frequently as solvents in asymmetric hydrogenations, we checked the stability of two tLANOP ligands in deuteriomethanol with ^1H and ^{31}P spectroscopy. For 4a no measurable decomposition was observed after 3 days at rt, whereas subsequent addition of water led to ca. 10% of hydrolysis after one more week. Under the same conditions the ligand 4f, which contains the bulky 3,5-*t*Bu₂-phenyl substituents, did not show any decomposition at all. As a comparison, oxoProNOP 3a was completely decomposed after 24 h in deuteriomethanol.

In addition, the stereochemical integrity of the tLANOP ligands was checked in order to rule out any partial racemization of the hydroxy amides (*R*)- and (*S*)-6 under the strongly basic phosphinylation conditions. For this purpose, (*S*)-4a, (*R*)-4b and (*R*)-4f, were hydrolyzed with methanolic HCl and 6 was recovered. GC analysis showed that the ee of 6 was unchanged with respect to the starting hydroxy amides used.

2.2. Synthesis of transition metal complexes

In order to establish unambiguously the absolute configuration of the tLANOP ligands, and in order to probe their chelating capability and the conformational properties of the chelates, the palladium complex (*R,S*)-10, the rhodium complex (*R*)-13a and the iridium complex (*S*)-13b were prepared.

The reaction of (*S*)-**4a** with $[\text{Pd}((R)\text{-dmphea})(\text{NCMe})_2]\text{BF}_4$ (*R*)-**9** ($\text{dmphea} = \eta^2\text{-Me}_2\text{NCHMe-CC}_5\text{H}_4$) in dichloromethane was carried out in analogy to published methods.^{10,11} If the reaction time was short (10 min at rt), the kinetic product was isolated in high yield (Scheme 2). X-Ray analysis of crystals grown at -30°C showed that this complex had the (*SP*-4-3) geometry of (*R,S*)-**10**. At longer reaction times, rearrangement of (*R,S*)-**10** to (*SP*-4-4)-(*R,S*)-**11** was observed. The latter, however, decomposed slowly in solution and could not be isolated.



Scheme 2.

The reaction of (*R*)-**4a** with **12a** or of (*S*)-**4a** with **12b**¹² afforded the cationic rhodium cyclooctadiene complex (*R*)-**13a** and the analogous iridium complex (*S*)-**13b**, respectively, in practically quantitative yield. A detailed investigation describing mono- and dinuclear rhodium complexes of **4a** will be published soon.¹³

2.3. Crystal structure of (*R,S*)-**10** and (*R*)-**13a**

ORTEP plots of the cationic components in (*R,S*)-**10** and (*R*)-**13a** are shown in Fig. 1. Table 4 (see Experimental section) shows experimental parameters for the structure determination. Both crystal structures confirmed the provisionally assigned absolute configuration of **4a** and indirectly that of **6**.

In both complexes the geometry around the metal atoms is distorted square-planar. In (*R,S*)-**10** the σ -coordinated carbon atom is located out of the palladium coordination plane by 0.493 \AA . In (*R*)-**13a**, if one takes the midpoints of the two coordinated olefinic bonds of cyclooctadiene as virtual monodentate ligands, the plane defined by them and rhodium forms an angle of 15.8° with the plane containing the two phosphorus atoms and rhodium.¹⁴ In spite of the different electronic and steric environments, however, the topology of the seven-membered chelate ring and the spatial arrangement of the phenyl groups of the PPh_2 moieties in **4a** in both (*R,S*)-**10** and mirror-inverted (*R*)-**13a** are practically identical (cf. data in Fig. 1). The twist-boat conformation of δ ((*R,S*)-**10**) or λ ((*R*)-**13a**) helicity is characterized by the quasi-planarity of the amido function bound at P(2) and by the location of the *t*-butyl group in pseudo-equatorial orientation. The phenyl substituents at the phosphorus atoms are in an alternating fashion pseudo-equatorially and pseudo-axially oriented. In both complexes the metal–P(N) is longer than the metal–P(O) bond, a phenomenon that seems to be general in transition metal complexes of amido-⁴ and aminophosphine-phosphinite ligands.¹⁵

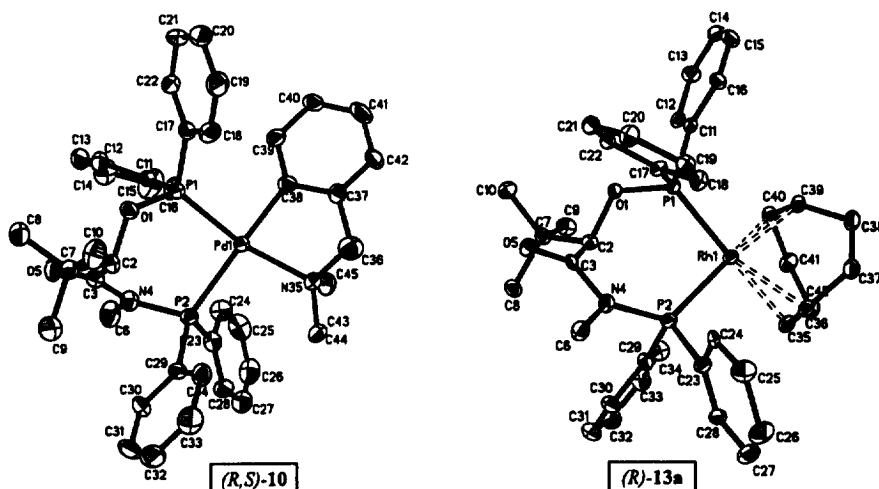


Figure 1. Molecular structures (30% thermal ellipsoids) with atom numbering scheme, selected bond lengths (Å), angles (°) and torsional angles (°). (*R,S*)-**10**: Pd(1)–P(1) 2.248(2), Pd(1)–P(2) 2.426(3), Pd(1)–N(35) 2.183(8), Pd(1)–C(38) 2.041(10), P(1)–O(1) 1.617(7), P(2)–N(4) 1.736(9); P(1)–Pd(1)–P(2) 94.53(9), C(38)–Pd(1)–N(35) 79.2(4), C(38)–Pd(1)–P(1) 89.5(3); C(2)–C(3)–N(4)–P(2) 5.3, O(5)–C(3)–N(4)–P(2) 179.9, Pd(1)–P(1)–O(1)–C(2) –32.5. (*R*)-**13a**: Rh(1)–P(1) 2.256(6), Rh(1)–P(2) 2.304(6), P(1)–O(1) 1.635(15), P(2)–N(4) 1.711(19), Rh–C(olefin) 2.18 and 2.20; P(1)–Rh(1)–P(2) 93.4(2); C(2)–C(3)–N(4)–P(2) 8.6, O(5)–C(3)–N(4)–P(2) 171.9, Rh(1)–P(1)–O(1)–C(2) 34.6

2.4. Asymmetric hydrogenations

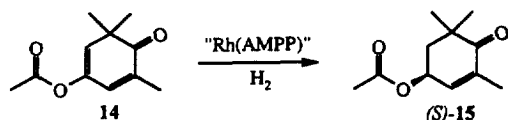
The tLANOP ligands were tested in the asymmetric hydrogenation of: (a) 4-oxoisophorone enol acetate **14** to (*S*)-phorenol acetate (*S*)-**15**, an intermediate in the synthesis of the natural pigment zeaxanthin¹⁶; and (b) the cyclic iminium salts **16a,b** to the octahydro-isoquinoline derivative (*S*)-**17**, the so-called (*S*)-octabase,¹⁷ an intermediate in the synthesis of the antitussivum dextromethorphan.

In the rhodium catalyzed asymmetric hydrogenation of **14**, the ee values achieved with the ligands of type **4** are at best moderate (Table 2, entries 1 and 2). In contrast, with one ligand of type **3** (**3b**, entry 5) 95% ee is reached. The latter result comes close to the so far best ee of 98% ee achieved in this hydrogenation with a DuPHOS-type diphosphine.¹⁸

In the iridium catalyzed asymmetric hydrogenation of the cyclic iminium salts **16a** and **16b**, increase of the steric encumbrance of the aryl substituents at the phosphorus atoms in the ligands **4a** and **4c–g** led to a remarkable improvement of the ee of **17**, e.g. from 4% with **4a** (Table 3, entry 7) to 78% with **4g** (entry 13) for the fluoroborate salt **16a** or even to 86% ee with **4f** (entry 18) for the bisulphate salt **16b**.¹⁹ Unfortunately, with these ligands the chemoselectivity was modest and substantial amounts of stereoisomeric decahydro-isoquinoline derivatives were formed as by-products. The two ligands of the oxoProNOP type tested (entries 14 and 15) gave higher chemoselectivity but low ees. With ligands of both type **3** and **4** the presence of cyclohexyl substituents on the phosphorus atoms brought about the highest chemoselectivity (96%) but, unfortunately, very low ees (entries 8, 15 and 17). Remarkably, these ligands with e.g. (*R*)-configuration afforded (*S*)-**17**, whereas those with aryl substituents afforded (*R*)-**17**.

In summary, we have shown that tLANOP ligands of type **4** can be readily prepared in high yields. Preliminary results indicate that they can be very efficient in asymmetric hydrogenation reactions. Their potential for other asymmetric catalytic reactions still remains to be explored.

Table 2
Asymmetric hydrogenation of 4-oxoisophorone enol acetate **14**^{a)}



Entry	Chiral ligand	no.	%ee ^{b)} (config)
1	(<i>R</i>)-Ph-tLANOP	4a	71 (<i>S</i>)
2	(<i>S</i>)-Cy-tLANOP	4b	71 (<i>R</i>)
3	(<i>S</i>)-(2-Furyl)-tLANOP	4c	5 (<i>S</i>)
4	(<i>S</i>)-Ph-oxoProNOP	3a	30 (<i>R</i>)
5	(<i>S</i>)-Cy-oxoProNOP	3b	95 (<i>R</i>)
6	(<i>S</i>)-(2-Furyl)-oxoProNOP	3c	31 (<i>R</i>)

^{a)} Hydrogenation conditions: [Rh(AMPP)]BF₄ prepared *in situ*, EtOAc, rt, 10 bar H₂, substrate-to-catalyst mole ratio (S/C) 100, 18h, complete conversion, cf. Experimental section for typical procedure.

^{b)} Enantiomeric excess determined by GC analysis, cf. Experimental section.

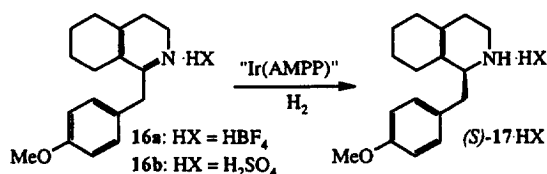
3. Experimental section

All manipulations of oxygen- and moisture-sensitive materials were conducted under an argon atmosphere. All solvents were distilled under argon before use. Hydrogen and argon were of 99.9999% purity. The complexes, [Ru(OAc)₂((*R*)- or (*S*)-BIPHEMP)] BIPHEMP=(6,6'-dimethylbiphenyl-2,2'-diyl)bis(diphenylphosphine),²⁰ were prepared according to reported procedures.⁶ The chlorophosphines were purchased or prepared according to known methods;²¹ their high purity was essential for obtaining the tLANOP ligands in high purity. The AMPP ligands **3a–c** were prepared according to a known general procedure.¹ Before use, basic alumina (Camag) was dried at 200°C under vacuum and stored under argon. Nuclear magnetic resonance spectra (NMR) were measured on a Bruker 250E (¹H 250 MHz and ³¹P 101.26 MHz) spectrometer in CDCl₃ using TMS (¹H) as an internal standard and 85% H₃PO₄ (³¹P) as an external standard. Optical rotations were measured on a Perkin–Elmer 241 spectrometer. Melting points were determined on a Büchi 510 and are uncorrected.

3.1. (*R*)-2-Hydroxy-3,3,N-trimethyl-butylamide (*R*)-6

In a glove box (O₂ content < 1 ppm) the catalyst solution was prepared by dissolving [Ru(OAc)₂((*R*)-BIPHEMP)] (385 mg, 0.50 mmol) in a 0.025 molar methanolic HCl solution (40 ml) and dichloromethane (40 ml) and stirring at rt for 1.5 h. This solution was transferred into a catalyst addition device. A 2 l Hastelloy autoclave was charged with **5**²² (71.6 g, 0.50 mol) and methanol (310 ml), then sealed, purged with argon and finally with hydrogen. The catalyst solution was allowed to flow into the autoclave with a slight overpressure and the hydrogenation was carried out at 60°C with a constant pressure of 60 bar. After 20 h the reaction mixture was drained off and evaporated. Crystallization of the crude residue from diisopropyl ether (250 ml) and cyclohexane (275 ml) at 5°C afforded (*R*)-**6** (43.9 g, 60.5%) as a white crystalline solid, mp 69–71°C. ¹H NMR (250 MHz, CDCl₃, 20°C): δ 0.99 (s, 9H, *t*Bu), 2.84 (d, 3H, NCH₃, *J*=5.0), 3.08 (d, 1H, OH, *J*=5.6), 3.71 (d, 1H, CHOH, *J*=5.6), 6.32 (b, 1H, NH). [α]_D²⁰ +61.0 (*c* 1, CHCl₃), ee=98.7% (determined by GC on an OV-61/p-DiMe-β-cyclodextrin chiral column).

Table 3
Asymmetric hydrogenation of 16·HX^{a)}



Entry	HX	AMPP ligand	no.	solvent ^{c)}	%select.	%ee ^{b)} (config)
7	HBF ₄	(S)-Ph- <i>t</i> LANOP	4a	MeOH/tol	64	4 (S)
8	"	(R)-Cy- <i>t</i> LANOP	4b	THF	96	22 (S)
9	"	(R)-(2-Furyl)- <i>t</i> LANOP	4c	THF	42	15 (R)
10	"	(S)-(Diphol)- <i>t</i> LANOP	4d	THF	30	13 (S)
11	"	(R)-(3,5-Xyl)- <i>t</i> LANOP	4e	MeOH/tol	76	5 (R)
12	"	(R)-(3,5- <i>t</i> Bu)- <i>t</i> LANOP	4f	MeOH/tol	50	72 (R)
13	"	(S)-(3,5- <i>t</i> Bu,4-MeO)- <i>t</i> LANOP	4g	MeOH/tol	55	78 (S)
14	"	(R)-Ph-oxoProNOP	3a	THF	83	27 (R)
15	"	(R)-Cy-oxoProNOP	3b	THF	96	11 (S)
16	H ₂ SO ₄	(S)-Ph- <i>t</i> LANOP	4a	THF/H ₂ O	40	19 (S)
17	"	(R)-Cy- <i>t</i> LANOP	4b	"	96	21 (S)
18	"	(S)-(3,5- <i>t</i> Bu)- <i>t</i> LANOP	4f	"	46	86 (S)
19	"	(S)-(3,5- <i>t</i> Bu,4-MeO)- <i>t</i> LANOP	4g	"	32	82 (S)

^{a)} Hydrogenation conditions: [Ir(Cl/T)(AMPP)] prepared in situ, rt, 100 bar H₂, S/C 25–100, 44 h, complete conversion, cf. Experimental section for typical procedure.

^{b)} Enantiomeric excess determined by GC analysis, cf. Experimental section. ^{c)} MeOH / toluene 1:1, THF / H₂O 40:1 (vol/vol).

MS (EI) *m/z* 146 (M⁺, 2%), 112 (M–H₂O–CH₃, 1%), 89 (M–C₄H₈, 100%). IR (KBr, ν, cm^{–1}): 1651 (b, C=O). Anal. calcd for C₇H₁₅NO₂: C, 57.90; H, 10.41; N, 9.65. Found: C, 57.97; H, 10.60; N, 9.61.

3.2. (S)-2-Hydroxy-3,3,N-trimethyl-butylamide (S)-6

The asymmetric hydrogenation of **5** (55 g, 0.384 mol) in the presence of [Ru(OAc)₂((S)-BIPHEMP)]/HCl (296 mg, 0.384 mmol) afforded, after crystallization, (S)-**6** (34.4 g, 62%) with mp 60–62°C, [α]_D²⁰ –59.9 (c 1, CHCl₃), ee=99.2%. Anal. found for C₇H₁₅NO₂: C, 58.02; H, 10.49; N, 9.59.

3.3. Preparation of *t*LANOP ligands 4a–g

3.3.1. (R)-Ph-*t*LANOP (R)-4a

In a typical experiment, (R)-**6** (3.88 g, 26.7 mmol) was dissolved in a 500 ml Schlenk tube containing THF (200 ml) and diisopropylamine (0.5 ml) and reacted at –78°C with *n*-butyllithium in hexane (28.5 ml, 53.5 mmol). After 1 h a solution of chlorodiphenylphosphine (11.8 g, 53.5 mmol) in THF (30 ml)

was added during 30 min and the mixture was stirred for 1 h. Then the cold bath was removed and the yellow clear solution evaporated. The residue was dried under high vacuum, taken up in diethyl ether and the suspension filtered under argon through basic alumina (60 g). The filter cake washed with diethyl ether (100 ml). The combined filtrates were evaporated and the residue dried under high vacuum. The resulting yellow oil was cooled to -180°C with liquid nitrogen, cold pentane (50 ml) was added and the mixture treated in an ultrasonic bath for 5 min, during which time white crystals formed. After 24 h at 5°C the supernatant was removed, the crystals were rinsed with pentane (2×20 ml, 0°C) and dried under high vacuum to afford (*R*)-**4a** (8.41 g, 61%) as a white crystalline solid, mp $95\text{--}96^{\circ}\text{C}$, $[\alpha]_{\text{D}}^{20} +37.5$ (*c* 1, CHCl_3). ^1H NMR (250 MHz, CDCl_3 , 20°C): δ 1.06 (s, 9H, *t*Bu), 2.73 (s, 3H, NCH_3), 5.86 (dd, 1H, $^3J_{\text{PH}}=^4J_{\text{PH}}=9.0$, CHO), 7.15–7.60 (m, 20H). MS (EI) m/z 514.3 ($\text{M}+\text{H}^+$, 90%). IR (KBr, ν , cm^{-1}): 1663 (s, C=O). Anal. calcd for $\text{C}_{31}\text{H}_{33}\text{NO}_2\text{P}_2$: C, 72.50; H, 6.48; N, 2.73; P, 12.06. Found: C, 72.45; H, 6.50; N, 2.50; P, 12.02.

The other *t*LANOP ligands with (*R*) or (*S*) configuration were prepared by procedures similar to that described for (*R*)-**4**, starting from the corresponding hydroxy amide and chlorophosphine.

3.3.2. (*S*)-*Ph-t*LANOP (*S*)-**4a**

10.6 g, 67% yield, colorless crystals, mp $95\text{--}96^{\circ}\text{C}$, $[\alpha]_{\text{D}}^{20} -37.7$ (*c* 1, CHCl_3). Anal. found for $\text{C}_{31}\text{H}_{33}\text{NO}_2\text{P}_2$: C, 72.42; H, 6.56; N, 2.46; P, 12.00.

3.3.3. (*R*)-*Cy-t*LANOP (*R*)-**4b**

Filtered through alumina in pentane, the residue after evaporation was not recrystallized. 8.20 g, 69% yield, colorless solid, moisture sensitive, $[\alpha]_{\text{D}}^{20} +18.8$ (*c* 1, CHCl_3). ^1H NMR (250 MHz, CDCl_3 , 20°C): δ 0.99 (s, 9H, *t*Bu), 1.0–2.2 (m, 44H, Cy), 2.89 (s, 3H, NCH_3), 5.26 (dd, 1H, $^3J_{\text{PH}}=^4J_{\text{PH}}=7.5$, CHO). MS (EI) m/z 537 (M^+ , 5%), 454 ($\text{M}^+-\text{C}_6\text{H}_{11}$, 50%). IR (KBr, ν , cm^{-1}): 1665 (s, C=O). Anal. calcd for $\text{C}_{31}\text{H}_{57}\text{NO}_2\text{P}_2$: C, 69.24; H, 10.68; N, 2.60; P, 11.52. Found: C, 69.12; H, 10.66; N, 2.54; P, 11.22.

3.3.4. (*S*)-*Cy-t*LANOP (*S*)-**4b**

Filtered through alumina in pentane, the residue after evaporation was not recrystallized. 4.20 g, 66% yield, colorless solid, moisture sensitive, $[\alpha]_{\text{D}}^{20} -18.9$ (*c* 1, CHCl_3). Anal. found for $\text{C}_{31}\text{H}_{57}\text{NO}_2\text{P}_2$: C, 68.92; H, 10.87; N, 2.41; P, 11.48.

3.3.5. (*R*)-(2-*Furyl*)-*t*LANOP (*R*)-**4c**

2.77 g, 48% yield, colorless solid. ^1H NMR (250 MHz, CDCl_3 , 20°C): δ 1.20 (s, 9H, *t*Bu), 3.12 (s, 3H, NCH_3), 5.9–6.1 (m, 6H), 6.5–7.3 (m, 7H). MS (EI) m/z 474.3 ($\text{M}+\text{H}^+$, 30%). IR (KBr, ν , cm^{-1}): 1681 (s, C=O). Anal. calcd for $\text{C}_{23}\text{H}_{25}\text{NO}_6\text{P}_2$: C, 58.35; H, 5.32; N, 2.96; P, 13.09. Found: C, 58.12; H, 5.29; N, 2.91; P, 12.93.

3.3.6. (*S*)-(Diphol)-*t*LANOP (*S*)-**4d**

4.74 g, 62% yield, colorless solid. ^1H NMR (250 MHz, CDCl_3 , 20°C): δ 1.19 (s, 9H, *t*Bu), 2.35 (s, 3H, NCH_3), 6.07 (dd, 1H, $^3J_{\text{PH}}=^4J_{\text{PH}}=8.7$, CHO). IR (KBr, ν , cm^{-1}): 1669 (s, C=O). Anal. calcd for $\text{C}_{31}\text{H}_{39}\text{NO}_2\text{P}_2$: C, 73.08; H, 5.74; N, 2.75; P, 12.16. Found: C, 72.79; H, 5.76; N, 2.88; P, 12.20.

3.3.7. (*R*)-(3,5-*Xyl*)-*t*LANOP (*R*)-**4e**

2.23 g, 73% yield, colorless solid. ^1H NMR (250 MHz, CDCl_3 , 20°C): δ 1.05 (s, 9H, *t*Bu), 2.15–2.50 (m, 24H), 2.78 (s, 3H, NCH_3), 5.82 (dd, 1H, $^3J_{\text{PH}}=^4J_{\text{PH}}=8.0$, CHO), 6.8–7.7 (m, 12H).

3.3.8. (R)-(3,5-*t*Bu)-*t*LANOP (R)-4f

3.78 g, 83% yield, colorless solid. ^1H NMR (250 MHz, CDCl_3 , 20°C): δ 1.10 (s, 9H, *t*Bu), 1.25–1.29 (4s, 72H, *t*Bu), 2.79 (s, 3H, NCH_3), 5.89 (dd, 1H, $^3J_{\text{PH}}=^4J_{\text{PH}}=8.7$, CHO), 7.2–7.6 (m, 12H). MS (ESI) m/z 963.3 ($\text{M}+\text{H}^+$, 25%). IR (KBr, ν , cm^{-1}): 1675 (s, C=O). Anal. calcd for $\text{C}_{63}\text{H}_{97}\text{NO}_2\text{P}_2$: C, 78.62; H, 10.16; N, 1.46; P, 6.44. Found: C, 77.72; H, 10.12; N, 1.36; P, 6.27.

3.3.9. (S)-(3,5-*t*Bu)-*t*LANOP (S)-4f

3.41 g, 55% yield, colorless solid. Anal. found for $\text{C}_{63}\text{H}_{97}\text{NO}_2\text{P}_2$: C, 78.32; H, 10.02; N, 1.38; P, 6.14.

3.3.10. (S)-(3,5-*t*Bu,4-MeO)-*t*LANOP (S)-4g

Filtered through alumina in pentane, the residue after evaporation was not recrystallized. 2.63 g, 60% yield, colorless solid, contains ca. 25% LiCl. ^1H NMR (250 MHz, CDCl_3 , 20°C): δ 1.03 (s, 9H, *t*Bu), 1.25–1.45 (m, 72H, *t*Bu), 2.77 (s, 3H, NCH_3), 3.64–3.70 (4×s, 12H, OCH_3), 5.76 (dd, 1H, $^3J_{\text{PH}}=^4J_{\text{PH}}=9.0$, CHO), 7.0–7.7 (m, 8H). MS (TSP) m/z 970.6 ($\text{M}-\text{tBu}-\text{OMe}$). IR (KBr, ν , cm^{-1}): 1673 (s, C=O). Anal. calcd for $\text{C}_{67}\text{H}_{105}\text{NO}_6\text{P}_2 \cdot 0.25\text{LiCl}$: C, 73.62; H, 9.68; N, 1.28; P, 5.67; Cl, 0.81. Found: C, 73.34; H, 9.82; N, 1.00; P, 5.63; Cl, 0.77.

3.4. [(SP-4-3)-Pd((R)-*dmphea*)(S)-4a)] BF_4 (R,S)-10

In a 50 ml Schlenk tube, a solution of $[\text{Pd}((\text{R})\text{-dmphea})(\text{NCMe})_2]\text{BF}_4$ (R)-9¹¹ (105 mg, 0.25 mmol) and (S)-4a (129 mg, 0.25 mmol) in dichloromethane (10 ml) was stirred for 10 min at rt. After evaporation, the residue was washed with diethyl ether (10 ml) and dried for 2 h under vacuum, affording (R,S)-10 (211 mg, 98%) as a colorless solid. ^1H NMR (250 MHz, CDCl_3 , 20°C): δ 0.67 (s, 9H, *t*Bu), 1.45 (bs, 3H, CHCH_3), 2.18, 2.27, 2.40 (3×m, 9H), 3.62 (m, 1H, CHCH_3), 5.04 (dd, 1H, $^3J_{\text{PH}}=6.3$, $^4J_{\text{PH}}=6.4$, CHO), 6.3–8.3 (m, 24 arom H). ^{31}P NMR (101.25 MHz): δ 73.3 (d, $J_{\text{PP}}=41$) (P–N); 136.6 (d, $J_{\text{PP}}=41$) (P–O). IR (KBr, ν , cm^{-1}): 1689 (m, C=O), 1084 (s, BF_4). Anal. calcd for $\text{C}_{41}\text{H}_{33}\text{BF}_4\text{NO}_2\text{P}_2\text{Pd}$: C, 57.60; H, 5.54; N, 3.28. Found: C, 56.42; H, 5.54; N, 3.08. Within 24 h at rt (R,S)-10 was completely converted to a mixture of (R,S)-11 (^{31}P NMR signals at 78.8 (d) and 122.2 (d), $J_{\text{PP}}=35$) and several by-products (main ^{31}P NMR signals at 37 (m) and 101–103 (m)). Attempts to isolate (R,S)-11 by crystallization resulted only in decomposition.

3.5. [Rh((R)-4a)(COD)] BF_4 (R)-13a

In a 100 ml Schlenk tube, to a suspension of $[\text{Rh}(\text{COD})_2]\text{BF}_4$ (144 mg, 0.355 mmol) in THF (10 ml) was added dropwise a solution of (R)-4a (189 mg, 0.368 mmol) in THF (10 ml). The orange-yellow solution was stirred for 5 min, evaporated and dried under high vacuum. The oily residue was stirred in diethyl ether and the supernatant removed. The solid residue was dried for 12 h in high vacuum, affording (R)-13a (278 mg, 97%) as a yellow crystalline material. ^1H NMR (250 MHz, CDCl_3 , 20°C): δ 0.90 (s, 9H, *t*Bu), 2.27 (d, 3H, NCH_3 , $J=5.7$), 2.2–2.6 (m, 8H), 4.38, 4.60, 4.76, 5.16 (4×bm, 4H, COD), 5.21 (dd, 1H, CHO, $^3J_{\text{PH}}=10.0$, $^4J_{\text{PH}}=5.0$), 7.2–8.2 (m, 20H). ^{31}P NMR (101.25 MHz): δ 83.4 (dd, $^1J_{\text{RhP}}=170$, $J_{\text{PP}}=25$) (P–N); 131.3 (dd, $^1J_{\text{RhP}}=167$, $J_{\text{PP}}=25$) (P–O). IR (KBr, ν , cm^{-1}): 1685 (m, C=O), 1083 (s, BF_4). Anal. calcd for $\text{C}_{39}\text{H}_{45}\text{BF}_4\text{NO}_2\text{P}_2\text{Rh}$: C, 57.73; H, 5.59; N, 1.73; P, 7.63. Found: C, 57.51; H, 5.59; N, 1.46; P, 7.41.

3.6. $[\text{Ir}((S)\text{-4a})(\text{COD})]\text{BF}_4$ (*S*)-13b

The analogous reaction of $[\text{Ir}(\text{COD})_2]\text{BF}_4$ with (*S*)-4a in THF afforded (*S*)-13b as a red crystalline material. ^1H NMR (250 MHz, CDCl_3 , 20°C): δ 0.84 (s, 9H, *t*Bu), 2.30 (d, 3H, NCH_3 , $J=6.3$), 2.0–2.6 (m, 8H), 4.05, 4.15, 4.40, 4.90 (4×bm, 4H, COD), 5.10 (dd, 1H, CHO, $^3J_{\text{PH}}=9.6$, $^4J_{\text{PH}}=4.0$), 7.2–8.1 (m, 20H). ^{31}P NMR (101.25 MHz): δ 71.0 (s) (P–N); 113.0 (s) (P–O). MS (ISP) m/z 814.5 (M^+). IR (KBr, ν , cm^{-1}): 1686 (m, C=O), 1083 (s, BF_4). Anal. calcd for $\text{C}_{39}\text{H}_{45}\text{BF}_4\text{NO}_2\text{P}_2\text{Rh}$: C, 52.00; H, 5.04; N, 1.56; P, 6.88. Found: C, 51.93; H, 4.95; N, 1.51; P, 6.43.

3.7. Hydrolysis of *t*LANOP ligands

A solution of (*S*)-4a (180 mg, 0.353 mmol) in dichloromethane (5 ml) was treated with water (1 ml), 25% HCl (0.1 ml) and methanol (1 ml). The mixture was stirred at rt for 1.5 h before sodium carbonate (3.2 g) was added and the suspension stirred for 30 min. After filtration the filtrate was evaporated and dried under vacuum to afford an oily residue consisting of a mixture of (*S*)-6 with 99.7% ee (GC analysis) and diphenylphosphine oxide. The analogous hydrolysis of (*R*)-4b afforded (*R*)-6 of 98.2% ee, that of (*R*)-4f afforded (*R*)-6 of 99.1% ee.

3.8. X-Ray structural analysis of (*R,S*)-10 and (*R*)-13a

Crystallographic data are summarized in Table 4. (*R,S*)-10: colorless crystals (0.3×0.3×0.2 mm) suitable for X-ray diffraction were grown by slow diffusion of a diethyl ether layer into a CH_2Cl_2 solution of (*R,S*)-10 at –30°C. 5669 independent reflections were measured at rt on a Siemens R3m/V diffractometer equipped with a graphite monochromator using Mo $\text{K}\alpha$ radiation. The θ range for data collection was 1.42–28.00°. (*R*)-13a: brick red crystals (0.4×0.3×0.25 mm) were grown by slow evaporation of a solution in $\text{CH}_2\text{Cl}_2/\text{Et}_2\text{O}$ at rt. 3466 independent reflections were measured at 173 K on a Siemens P4 diffractometer equipped with a Siemens rotating anode M18XHF and a graphite monochromator using Cu $\text{K}\alpha$ radiation. The θ range for data collection was 4.28–63.94°. ²³ For the refinement, 444 restraints were used. The Flack parameter was refined to 0.09(4), supporting the established absolute configuration. Both structures were solved by direct methods and all non-hydrogen atoms were refined anisotropically (with the exception of (*R*)-13a, where the solvent molecule and the counterion were refined isotropically) using full-matrix least-square technique and Fourier synthesis based on F^2 (SHELX-package). ²⁴ H atoms were constrained in the calculated positions.

3.9. Asymmetric hydrogenation of 14

In a glove box a solution of $[\text{Rh}(\text{COD})_2]\text{BF}_4$ (11.4 mg, 0.051 mmol) and (*R*)-4a (13.1 mg, 0.051 mmol) in ethyl acetate (6.5 ml) was stirred for 60 min, after which time 14 (0.50 g, 2.57 mmol) was added. The autoclave was removed from the box and the hydrogenation carried out under 10 bar of hydrogen and at rt for 18 h. After evaporation of the solvent, a sample of the crude ester 15 was converted to the alcohol (NaOMe/MeOH, 30 min, 50°C) and, after addition of few drops of acetic acid, analyzed by GC (column: OV-61/*p*-DiMe- β -CD). The ee of (*S*)-15 was 71%.

Table 4
Crystal data

compound	(<i>R,S</i>)- 10	(<i>R</i>)- 13a
formula	C ₄₁ H ₄₇ N ₂ O ₂ P ₂ PdBF ₄	C ₃₉ H ₄₅ NO ₂ P ₂ RhBF ₄ ·CH ₂ Cl ₂
cryst syst	orthorhombic	tetragonal
space group	P2 ₁ 2 ₁ 2 (no. 18)	P4 ₁ (no. 76)
<i>a</i> , Å	19.905(4)	10.319(4)
<i>b</i> , Å	20.587(4)	10.319(4)
<i>c</i> , Å	10.333(2)	37.554(17)
<i>V</i> , Å ³	4234(14)	3999(3)
<i>Z</i>	4	4
ρ_{calcd} , g cm ⁻³	1.341	1.489
<i>F</i> (000)	1760	1840
residual <i>R</i> , <i>R</i> _w ^a	0.0621, 0.1818	0.1137, 0.2728
for <i>I</i> > 2 σ		

3.10. Asymmetric hydrogenation of **16a**

In a glove box a solution of [IrCl(COD)]₂ (13.4 mg, 0.020 mmol), (*R*)-**4f** (57.7 mg, 0.060 mmol) and tetrabutylammonium iodide (59.1 mg, 0.16 mmol) in toluene (4 ml) was stirred for 30 min, after which time **16a** (0.343 g, 1.0 mmol) and methanol (4 ml) were added. The autoclave was removed from the box and the hydrogenation carried out under 100 bar of hydrogen and at rt for 44 h. Evaporation of the solvent and basic work-up afforded crude (*R*)-**17**, which was converted to the amide of (–)-camphanic acid (DCC, DMAP, CH₂Cl₂, 60°C, 30 min). GC analysis (column: OV-240 OH, Ohio Valley Chemicals, Marietta, OH) showed the conversion to be complete. The ee of (*R*)-**17** was 72% and the chemoselectivity 48%.

Acknowledgements

We wish to thank our colleagues from the Analytical Services for NMR Spectra (Dr. W. Arnold), elemental analyses (Dr. S. Müller), GC analyses (Dr. W. Walther), P. Schönholzer for the X-ray structure determinations and Dr. D. Bur for molecular modeling calculations. We also thank M. Glatz, A. Meili, D. Spiess and J. Stadelmann for skillful technical assistance and Dr. Y. Cramer for helpful discussions.

References

1. Roucoux, A.; Agbossou, F.; Mortreux, A.; Petit, F. *Tetrahedron: Asymmetry* **1993**, *4*, 2279.
2. Carpentier, J.-F.; Mortreux, A. *Tetrahedron: Asymmetry* **1997**, *8*, 1083 and references therein.
3. Ait Ali, M.; Alloud, S.; Karim, A.; Roucoux, A.; Mortreux, A. *Tetrahedron: Asymmetry* **1995**, *6*, 369.
4. Roucoux, A.; Thieffry, L.; Carpentier, J.-F.; Devocelle, M.; Méliet, C.; Agbossou, F.; Mortreux, A.; Welch, A. J. *Organometallics* **1996**, *15*, 2440.
5. The preferred calculated conformation of **4a** in a hypothetical cationic rhodium complex was practically identical to that determined later in **10** and **13a** by X-ray (D. Bur, unpublished results).
6. Heiser, B.; Broger, E. A.; Cramer, Y. *Tetrahedron: Asymmetry* **1991**, *2*, 51.
7. Kitamura, M.; Ohkuma, T.; Inoue, S.; Sayo, N.; Kumobayashi, H.; Akutagawa, S.; Ohta, T.; Takaya, H.; Noyori, R. *J. Am. Chem. Soc.* **1988**, *110*, 629.
8. Noyori, R. *Asymmetric Catalysis in Organic Synthesis*, John Wiley & Sons, Inc., 1994.
9. Allen, W. D.; Taylor, B. F. *J. Chem. Soc., Dalton Trans.* **1982**, 51.
10. (a) Roberts, N. K.; Wild, S. B. *J. Am. Chem. Soc.* **1979**, *101*, 6254; (b) *J. Chem. Soc., Dalton Trans.* **1979**, 2015; (c) Otsuka, S.; Nakamura, A.; Kano, T.; Tani, K. *J. Am. Chem. Soc.* **1971**, *93*, 4301; (d) Tani, K.; Brown, L. D.; Ahmed, J.; Ibers, J. A.; Yokota, M.; Nakamura, A.; Otsuka, S. *ibid.* **1977**, *99*, 7876.
11. Fornies, J.; Navarro, R.; Sicilia, V. *Polyhedron* **1988**, *28*, 219. During the preparation of the manuscript, the following cognate papers appeared: Falvello, L. R.; Fernandez, S.; Navarro, R.; Pascual, I.; Urriolabeitia, E. P. *J. Chem. Soc., Dalton Trans.* **1997**, 763; and Barco, I. C.; Falvello, L. R.; Fernandez, S.; Navarro, R.; Urriolabeitia, E. P. *J. Chem. Soc., Dalton Trans.* **1998**, 1699.
12. Schrock, R. R.; Osborn, J. A. *J. Am. Chem. Soc.* **1971**, *93*, 2397.
13. Feiken, N.; Pregosin, P.; Trabesinger, G. to be published in *Organometallics*, **1998**.
14. Armstrong, S. K.; Brown, J. M.; Burk, M. J. *Tetrahedron Lett.* **1993**, *34*, 879.
15. (a) Naili, S.; Carpentier, J.-F.; Agbossou, F.; Mortreux, A.; Nowogrocki, G.; Wignacourt, J.-P. *Organometallics* **1995**, *14*, 401. (b) Cesarotti, E.; Chiesa, A.; Ciani, G.; Sironi, A. *J. Organomet. Chem.* **1983**, *251*, 79.
16. Mayer, H. *Pure & Appl. Chem.* **1979**, *51*, 535.
17. (a) Den Hollander, C. W.; Leimgruber, W.; Mohacs, E. Ger. Offen. DE 2003486 to F. Hoffmann-La Roche Ltd, August 13, 1970, CAN 73:77081. (b) Imwinkelried, R. *Chimia* **1997**, *51*, 300.
18. (a) Broger, E. A.; Cramer, Y.; Schmid, R.; Siegfried, T. EP 691325 A1 960110 to F. Hoffmann-La Roche AG, CAN 124:260450. (b) Scalone, M. *ChiraTech* 97, Philadelphia, PA, 11–13 November 1997.
19. Broger, E. A.; Scalone, M.; Wehrli, C. EP 850931 A2 980701 to F. Hoffmann-La Roche AG, CAN 129:109000.
20. Schmid, R.; Cereghetti, M.; Heiser, B.; Schönholzer, P.; Hansen, H.-J. *Helv. Chim. Acta* **1988**, *71*, 897.
21. RajanBabu, T. V.; Casalnuovo, A. L.; Ayers, T. *J. Am. Chem. Soc.* **1994**, *116*, 9869.
22. Seifert, D.; Hui, R. C. *Tetrahedron Lett.* **1984**, *25*, 5251.
23. The high correlation coefficients in the crystal structure of (*R*)-**13a** reflect the rather poor quality of the crystal and the errors due to absorption effects (use of the Cu-radiation). Moreover, the solvent molecule (CH₂Cl₂) and the counterion (BF₄[−]) show some degree of disorder. Therefore, the somewhat weaker quality of the structural analysis should not affect the correctness of the structure of (*R*)-**13a**.
24. Sheldrick, G. M. *Acta Crystallography Section A* **1990**, *46*, 467.